Journal of Neurology
https://doi.org/10.1007/s00415-022-11494-0

ORIGINAL COMMUNICATION

Neural correlates of digital measures shown by structural MRI: a post-hoc analysis of a smartphone-based remote assessment feasibility study in multiple sclerosis

Marco Ganzetti[1] · Jennifer S. Graves[2] · Sven P. Holm[1] · Frank Dondelinger[1,6] · Luciana Midaglia[3,4] · Laura Gaetano[1] · Licinio Craveiro[1] · Florian Lipsmeier[1] · Corrado Bernasconi[1] · Xavier Montalban[3,4] · Stephen L. Hauser[5] · Michael Lindemann[1]

Received: 20 June 2022 / Revised: 15 November 2022 / Accepted: 17 November 2022
© The Author(s) 2022

Abstract

Background A study was undertaken to evaluate remote monitoring via smartphone sensor-based tests in people with multiple sclerosis (PwMS). This analysis aimed to explore regional neural correlates of digital measures derived from these tests.

Methods In a 24-week, non-randomized, interventional, feasibility study (NCT02952911), sensor-based tests on the Floodlight Proof-of-Concept app were used to assess cognition (smartphone-based electronic Symbol Digit Modalities Test), upper extremity function (Draw a Shape Test, Pinching Test), and gait and balance (Static Balance Test, Two-Minute Walk Test, U-Turn Test). In this post-hoc analysis, digital measures and standard clinical measures (e.g., Nine-Hole Peg Test [9HPT]) were correlated against regional structural magnetic resonance imaging outcomes. Seventy-six PwMS aged 18–55 years with an Expanded Disability Status Scale score of 0.0–5.5 were enrolled from two different sites (USA and Spain). Sixty-two PwMS were included in this analysis.

Results Worse performance on digital and clinical measures was associated with smaller regional brain volumes and larger ventricular volumes. Whereas digital and clinical measures had many neural correlates in common (e.g., putamen, globus pallidus, caudate nucleus, lateral occipital cortex), some were observed only for digital measures. For example, Draw a Shape Test and Pinching Test measures, but not 9HPT score, correlated with volume of the hippocampus ($r = 0.37$ [drawing accuracy over time on the Draw a Shape Test]/-0.45 [touching asynchrony on the Pinching Test]), thalamus ($r = 0.38/-0.41$), and pons ($r = 0.35/-0.35$).

Conclusions Multiple neural correlates were identified for the digital measures in a cohort of people with early MS. Digital measures showed associations with brain regions that clinical measures were unable to demonstrate, thus providing potential novel information on functional ability compared with standard clinical assessments.

Keywords Multiple sclerosis · Smartphone sensor · MRI · Neural correlates · Digital health technology tools

✉ Florian Lipsmeier
florian.lipsmeier@roche.com

1 F. Hoffmann-La Roche Ltd, Basel, Switzerland

2 Department of Neurosciences, University of California San Diego, San Diego, CA, USA

3 Department of Neurology-Neuroimmunology, Centre d'Esclerosi Múltiple de Catalunya (Cemcat), Hospital Universitari Vall d'Hebron, Barcelona, Spain

4 Department of Medicine, Autonomous University of Barcelona, Barcelona, Spain

5 Department of Neurology, University of California San Francisco, San Francisco, CA, USA

6 Present Address: Novartis Institutes for Biomedical Research, Basel, Switzerland

Published online: 05 December 2022

Introduction

Multiple sclerosis (MS) is a chronic disease of the central nervous system [1]. A long-held view of MS is of a multifocal, immune-mediated, inflammatory-demyelinating, and degenerative disorder of the white matter. Recent structural magnetic resonance imaging (MRI) studies, however, have revived the important role of cortical pathology in the pathophysiology of MS and in the rate of disability progression [2].

MRI-measured atrophy occurs in distinct, non-random patterns and involves many different regions, including the cerebral cortex, deep gray matter, brainstem, cerebellum, and spinal cord [2–7]. The rate of atrophy differs from region to region [6]. However, the progression of regional atrophy tends to follow specific sequences depending on the MS phenotype. In relapse-onset MS, the first regions affected by atrophy include the posterior cingulate cortex and precuneus, while the globus pallidus and medial precentral gyrus are among the last regions to become atrophic. In primary progressive MS, by comparison, the first regions to become atrophic are the thalamus, cuneus, and precuneus, and the last regions to show signs of atrophy are the frontal operculum and middle temporal gyrus [7].

Although there have been efforts to link clinical disability to regional atrophy [8–12], the relationship between digital measures of functional ability and MRI outcomes has not been extensively studied. Previously we showed that digital measures obtained with the Floodlight Proof-of-Concept (PoC) app in people with MS (PwMS) correlate with global MRI outcomes, in particular with total brain volume [13]. However, this analysis did not consider the regional specificity of cortical, deep gray matter, infratentorial, and spinal cord pathology. Here we extend this prior work by assessing the regional neural correlates of an expanded set of digital measures.

Methods

Study design and participants

This 24-week, non-randomized, interventional, feasibility study (clinicaltrials.gov: NCT02952911) aimed to assess the feasibility of remotely monitoring PwMS with the Floodlight PoC app, through sensor-based assessment via a provisioned smartphone device [14]. The study design, inclusion, and exclusion criteria have been previously reported [13, 14]. The study enrolled 76 PwMS and 25 healthy controls aged 18–55 years, from two separate sites in the USA (University of California San Francisco, San Francisco, CA) and Spain (Multiple Sclerosis Centre of Catalonia, Vall d'Hebron University Hospital, Barcelona); MRI data were only collected from PwMS. PwMS were diagnosed according to the 2010 revised McDonald criteria [15] and had an Expanded Disability Status Scale (EDSS) [16] at baseline of 0.0–5.5. A sample size of least 70 PwMS was considered adequate to detect a linear correlation coefficient of 0.33 with > 80% power.

Floodlight PoC app

At baseline, all participants received a pre-configured smartphone (Samsung Galaxy S7) with the Floodlight PoC app pre-installed [13, 14]. The app prompted all participants to perform daily and weekly sensor-based tests of functional ability (referred to as "active tests") at home without supervision by a physician or nurse, in three key domains affected by MS. Cognition was assessed by the smartphone-based electronic Symbol Digit Modalities Test (e-SDMT), upper extremity function by the Draw a Shape Test and Pinching Test, and gait and balance by the Static Balance Test (SBT), Two-Minute Walk Test (2MWT), and U-Turn Test (UTT) (Fig. 1). Performance on each active test was quantified by a set of digital measures extracted from the sensor signals that are illustrative of the test (Table 1).

Smartphone sensor-based tests

Key neurologic functions underlying cognitive information processing speed were assessed by the e-SDMT. It instructed participants to correctly match as many symbols as possible to their paired digits within 90 s, according to a symbol–digit key also displayed on the smartphone screen.

The Draw a Shape Test assessed fine finger movements, or dexterity; participants were prompted to draw six prewritten shapes of increasing complexity (two diagonal lines, a square, a circle, a figure-of-8, and a spiral). By comparison, the Pinching Test measured fine pinching or grasping dexterity. Participants were instructed to successfully pinch as many circular tomatoes appearing on the screen as possible within 30 s, with new tomatoes appearing at random locations.

Finally, gait and balance were assessed by three active tests: the SBT, 2MWT, and UTT. The SBT required participants to stand as still as possible for 30 s. The 2MWT assessed regular, straight walking for 2 min. The UTT, which measured both dynamic balance and gait, instructed participants to perform five consecutive U-turns that were at least 4 m apart, within a minute. The use of an assistive device and/or orthotic was permitted as needed while performing the 2MWT and UTT.

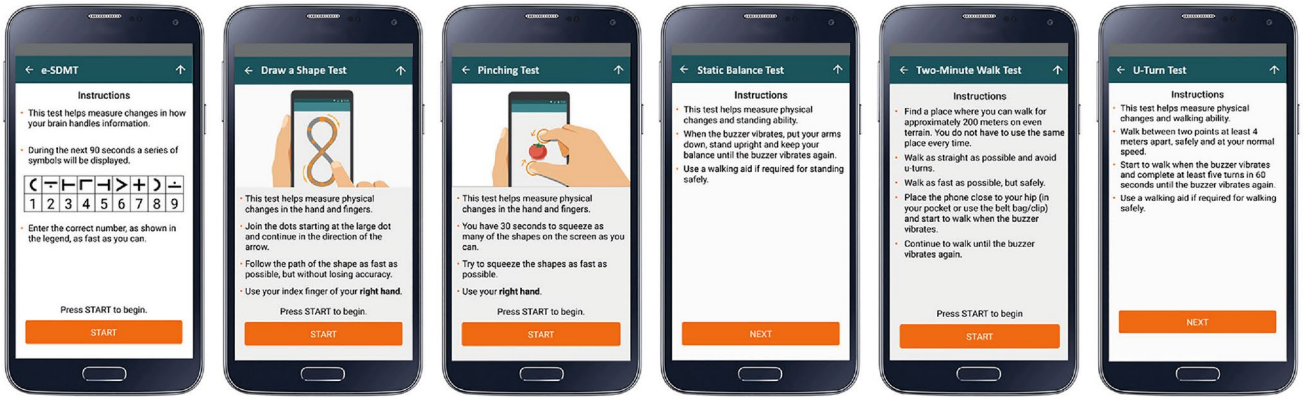

Fig. 1 Screenshots of the smartphone sensor-based tests included in the Floodlight PoC app. Screenshots depict the instruction screens for the smartphone-based electronic Symbol Digit Modalities Test, Draw a Shape Test, Pinching Test, Static Balance Test, Two-Minute Walk Test, and U-Turn Test. *e-SDMT* smartphone-based electronic Symbol Digit Modalities Test, *PoC* Proof-of-Concept

Digital data processing

Since the active tests were unsupervised, quality control flags as defined in Montalban et al. [13] were applied to identify tests that were not performed in accordance with the test's instructions and to ensure accurate interpretation of the collected data. This included flags to identify attempts of "play to quit" (i.e., trying to complete an active test as quickly as possible without performing the instructed tasks) or instances where the smartphone device was kept on a table during the gait and balance tests. Any test identified by one of these flags was excluded from the analyses. All remaining tests were considered as valid tests. Only participants who contributed on average at least 1.5 valid tests per week (corresponding to 21% adherence) were included in the analysis.

MRI acquisition and processing

Image acquisition

Brain MRI scans were collected from PwMS at baseline and at week 24 with Siemens 3-Tesla scanners (Siemens Healthcare GmbH, Erlangen, Germany) following optimized clinical practice protocols in place at the two investigating centers: (1) Hospital Universitari Vall d'Hebron, three-dimensional (3D) T1-weighted (repetition time [TR] = 2300 ms; echo time [TE] = 2.98 ms; inversion time [TI] = 900 ms; voxel size = 1 × 1 × 1 mm) fluid-attenuated inversion recovery (FLAIR; TR = 6000 ms; TE = 394 ms; TI = 2100 ms; voxel size = 1 × 1 × 1 mm) sequences acquired in a Siemens Trio Tim; (2) University of California San Francisco, 3D T1-weighted (TR = 2300 ms; TE = 2.98 ms; TI = 900 ms; voxel size = 1 × 1 × 1 mm) FLAIR (TR = 5000 ms; TE = 389 ms; TI = 1,800 ms; voxel size = 1 × 1 × 1 mm) sequences acquired in a Siemens Skyra.

Image processing

MR images were analyzed with icobrain ms v.5.0 (icometrix, Leuven, Belgium), a CE- and Food and Drugs Administration-certified software as medical device for automatic labeling, visualization, and volumetric quantification of segmentable brain structures [17–20], which combines two sequential pipelines. (1) An automated method for white matter lesion segmentation that uses 3D T1-weighted and FLAIR MR images in a probabilistic model. The accuracy and reproducibility of this software has been shown to be comparable to other well-established MS lesion segmentation algorithms (e.g., Lesion-TOADS, Lesion Segmentation Tool [17, 18]); (2) An automated multi-atlas cortical and subcortical segmentation method, which showed similar accuracy and reproducibility to commonly used automatic segmentation tools [21, 22]. Icobrain ms allowed extraction of normalized volumes for 34 anatomical regions, including cerebral gray matter regions ($n = 20$), deep gray matter regions ($n = 7$), brainstem ($n = 3$), cerebellum ($n = 2$), lateral ventricles ($n = 1$), and cerebral white matter ($n = 1$). In addition, icobrain ms allowed calculation of the corpus callosum area ($n = 1$) and upper cervical cord area ($n = 1$). As the cervical spinal cord was within the field of view on brain scans, the mean upper cervical cord area along C2–C3 levels was computed from the brain images [23, 24] using the icobrain ms fully automated pipeline [25, 26] based on the Spinal Cord Toolbox [27] (see Table 1 for more details). After visual inspection of the segmentation output, no participants were excluded from the analyses due to low quality MRI data or unsuccessful segmentation outputs.

Table 1 Outcome variables

Floodlight PoC app				
Functional domain	Smartphone sensor-based active test	Functional subdomain	Digital measure[a]	Higher scores indicate performance that is:
Upper extremity function	Draw a Shape Test	Accuracy	Mean trace accuracy	Better
		Swiftness of movement	Mean trace celerity, 1/s	Better
		Smoothness of movement	CV of linear, angular, and radial drawing velocity	Worse
	Pinching Test	Accuracy	Total number of successful pinches, *n*	Better
		Responsiveness	Gap time between pinch attempts, s	Worse
		Pinching asynchrony	Double touch asynchrony of successful pinches, s	Worse
Cognition	e-SDMT	Information processing speed	Number of correct responses, *n*	Better
			Maximum gap time between correct responses, s	Worse
		Cognitive fatigue	Speed fatigability index of the last 30 s	Better
Gait and balance	SBT	Postural control	Sway path, m/s^2	Worse
	UTT	Turning ability (dynamic balance and gait)	Turn speed, rad/s	Better
	2MWT	Gait pace	Step frequency, Hz	Better
		Gait variability	Step frequency variance, Hz^2	Worse
		Gait intensity	Step power, m^2/s^3	Better

Normalized volumes derived from brain MRI scans, mL[b]			
Cerebral cortex gray matter	Deep gray matter	Brainstem and upper cervical cord area	Other
1. Middle frontal	1. Thalamus	1. Midbrain	1. Lateral ventricles
2. Superior frontal	2. Hippocampus	2. Pons	2. Cerebral white matter
3. Lateral and medial orbitofrontal	3. Putamen	3. Medulla oblongata	3. Corpus callosum area
4. Precentral	4. Globus pallidus	4. Upper cervical cord area[c]	4. Cerebellum—hemispheres
5. Postcentral	5. Caudate nucleus		5. Cerebellum—vermis
6. Paracentral	6. Amygdala		
7. Opercularis, triangularis, orbitalis	7. Accumbens		
8. Insula			
9. Precuneus			
10. Cuneus, pericalcarine, lingual			
11. Anterior cingulate			
12. Posterior cingulate			
13. Isthmus cingulate			
14. Parahippocampus, fusiform, entorhinal			
15. Superior parietal			
16. Supramarginal			
17. Inferior parietal			
18. Lateral occipital			
19. Inferior and middle temporal			
20. Superior and transverse temporal			

2MWT Two-Minute Walk Test, *e-SDMT* smartphone-based electronic Symbol Digit Modalities Test, *PoC* Proof-of-Concept, *SBT* Static Balance Test, *UTT* U-Turn Test

[a]Computational definitions are provided in Table SI1

[b]Volumes were calculated for all regions with the exception of the corpus callosum and the upper cervical cord for which areas measured in mm^2 were calculated

[c]Upper cervical cord area was determined as mean area along C2–C3 levels

Standard clinical measures

During three clinical visits (baseline, week 12, and week 24) PwMS underwent clinical evaluation. These included the oral Symbol Digital Modalities Test (SDMT), Nine-Hole Peg Test (9HPT), Berg Balance Scale, Timed 25-Foot Walk (T25FW), and EDSS.

Statistical analysis

Due to the exploratory nature of this analysis, an unbiased approach with no pre-specified hypotheses was adopted to investigate associations between the brain/spinal cord regions and the digital measures obtained with the Floodlight PoC app (Table 1) and the standard clinical measures. Two separate cross-sectional analyses were conducted on the digital measures and, for comparison, on the standard clinical measures. First, these measures were correlated against regional, structural MRI outcomes using Spearman's rank correlation. Since the digital measures may be confounded by age, sex, and body mass index, the correlation analysis was adjusted for these confounders with a robust linear model via iteratively reweighted least squares [28]. Statistical significance was set at $q < 0.05$ after applying the false discovery rate (FDR) correction to correct for multiple comparisons for each digital and standard clinical measure separately [29].

In the second analysis, the variance in the digital measures that can be explained by volumetric MRI data was estimated. Here, a Bayesian ridge regression model [30] with leave-one-out cross validation was used to estimate the R^2 score, i.e., a measure related to the proportion of the variance in the dependent variable (digital measure or standard clinical measure) that is predictable from the independent variables (structural MRI outcomes). The following two models were considered: (1) the univariate Whole Brain model, which included the normalized total brain volume to estimate the variance in the digital measures and standard clinical measures; (2) the multivariate Parcellation model, which instead included the normalized volume and cross-sectional area measurements of 36 MRI regions.

Given the relatively short duration of the study (24 weeks) and the stability of the clinical and MRI measures over the study period (Fig. SI1), a data aggregation approach was followed to reduce variability and to deal more effectively with missing data. For both analyses, the data were aggregated as follows: for the digital measures, the median across all valid active tests was calculated; for the standard clinical measures and MRI outcomes, the mean of the three clinical visits (baseline, week 12, and week 24) and two MRI scans (baseline and week 24), respectively, were calculated.

All statistical analyses were performed in Python 3.7.9 (www.python.org) using statsmodels 0.12.0, an open-source module for data analysis and scientific computing (www.statsmodels.org).

Results

The study enrolled 76 PwMS between November 28, 2016 and November 13, 2017 (study completion date was May 4, 2018), of which 62 (82%) PwMS were included in the analyses presented here, comprising of 11 PwMS from the University of California San Francisco and 51 PwMS from the Hospital Universitari Vall d'Hebron. Of the 14 excluded PwMS, 12 were excluded for poor adherence to the active tests and two for missing MRI scans. Full baseline demographics and disease characteristics have been previously published [14] and those included in the current analyses are provided in Table 2. Of those PwMS included, 68% were female, mean age was 39.7 years (standard deviation [SD] 7.5), mean EDSS at baseline was 2.5 (SD 1.4; range 0.0–5.5), and 89% were diagnosed with relapsing–remitting MS. In order to exclude any potential effect of the MS phenotype on volumetric MRI data, we compared all 36 regions of interest between the groups of people with relapsing–remitting MS and progressive MS. As reported in Fig. SI2, significant differences were observed in only one of the 36 regions (combined occipital regions of cuneus, lingual gyrus, and pericalcarine cortex). This suggests that regional volumes were not dissimilar across relapsing and progressive MS phenotypes in this cohort. Additionally, no significant changes between the two study sites were found for age ($p = 0.846$), sex ($p = 0.145$), body mass index ($p = 0.905$), and disease phenotype ($p = 0.436$) (Fig. SI3).

The regional neural correlates of the digital measures and the standard clinical measures are summarized in Fig. 2. Uncorrected p values and the respective FDR-corrected p values (q values) are reported in the supplementary appendix (Fig. SI4 and SI5). Brain maps highlighting the statistically significant correlations after FDR correction are provided in Fig. 3. Higher EDSS scores correlated with smaller volumes of the cerebral white matter ($r = -0.42$, $q < 0.05$), lateral occipital lobe ($r = -0.43$, $q < 0.05$), insula ($r = -0.37$, $q < 0.05$), putamen ($r = -0.36$, $q < 0.05$), and globus pallidus ($r = -0.38$, $q < 0.05$).

The e-SDMT and oral SDMT showed a similar correlation pattern with regional MRI outcomes (Figs. 2, 3a). On both, a lower number of correct responses was significantly associated with smaller volumes of the cerebral white matter ($r = 0.49$ for e-SDMT/$r = 0.47$ for oral SDMT), corpus callosum ($r = 0.39/0.40$, $q < 0.05$), postcentral gyrus ($r = 0.33/0.34$, $q < 0.05$), lateral occipital lobe ($r = 0.38/0.30$, $q < 0.05$), insula ($r = 0.35/0.39$, $q < 0.05$), superior and transverse temporal gyrus ($r = 0.37/0.48$, $q < 0.05$), paracentral

Table 2 Baseline demographics and disease characteristics

Variable	PwMS cohort included in the analyses ($n=62$)
Site	11 (USA), 51 (Spain)
Female, *n*/*N* (%)	42/62 (67.7)
Age, years, mean (SD)	
Mean (SD)	39.7 (7.5)
Min.–Max.	20–57
BMI, kg/m^2	
Mean (SD)	24.4 (4.4)
Min.–Max.	17.1–37.6
Diagnosis, *n* (%)	
RRMS	55 (89)
PPMS	3 (5)
SPMS	4 (6)
Disease duration at baseline, years	
Mean (SD)	9.5 (6.6)
Min.–Max.	0.7–24.9
Normalized total brain volume, mL	
Mean (SD)	1471.9 (65.0)
Min.–Max.	1277.1–1628.1
EDSS	
Mean (SD)	2.5 (1.4)
Min.–Max.	0.0–5.5
Oral SDMT, number of correct responses	
Mean (SD)	53.4 (11.7)
Min.–Max.	26–77
9HPT, seconds	
Mean (SD)	22.4 (4.3)
Min.–Max.	16.4–40.3
T25FW, seconds	
Mean (SD)	6 (2)
Min.–Max.	3.6–12.5
Berg Balance Scale, total score	
Mean (SD)	52.4 (5.8)
Min.–Max.	31–56

9HPT Nine-Hole Peg Test, *BMI* body mass index, *EDSS* Expanded Disability Status Scale, *PPMS* primary progressive multiple sclerosis, *PwMS* people with multiple sclerosis, *RRMS* relapsing–remitting multiple sclerosis, *SD* standard deviation, *SDMT* Symbol Digit Modalities Test, *SPMS* secondary progressive multiple sclerosis, *T25FW* Timed 25-Foot Walk

gyrus ($r=0.35/0.36$, $q<0.05$), and deep gray matter structures such as the thalamus, putamen, globus pallidus, and caudate nucleus ($r=0.37–0.51/0.51–0.60$, $q<0.05$). A lower number of correct responses on either test was also associated with a larger volume of the lateral ventricles ($r=-0.50/-0.57$, $q<0.05$). Two correlations were only observed on the e-SDMT, but not on the oral SDMT. This included the correlation between the e-SDMT number of correct responses and the volume of the cuneus, pericalcarine cortex, lingual gyrus ($r=0.34$, $q<0.05$), and between the e-SDMT maximum gap duration between correct responses and the volume of the superior frontal lobe ($r=-0.37$, $q<0.05$).

Likewise, for each regional MRI outcome that showed significant correlation with the 9HPT there was at least one Draw a Shape Test measure that was significantly correlated with the same MRI outcome (Figs. 2, 3b, SI6a). Worse performance on either test was associated with smaller volumes of the cerebral white matter ($|r|=0.33–0.41$, $q<0.05$), lateral occipital lobe ($|r|=0.39–0.47$, $q<0.05$), and deep gray matter nuclei such as the putamen, globus pallidus, caudate nucleus, and accumbens ($|r|=0.31–0.44$, $q<0.05$), as well as a larger volume of the lateral ventricles ($|r|=0.38–0.45$, $q<0.05$). However, some correlates were only observed on the Draw a Shape Test, but not the 9HPT. For example, mean trace celerity correlated with volumes of the thalamus ($r=0.38$, $q<0.05$), hippocampus ($r=0.37$, $q<0.05$), and isthmus cingulate ($r=-0.37$, $q<0.05$). Velocity-based measures of round shapes correlated with volumes of the thalamus ($|r|=0.35–0.43$, $q<0.05$), hippocampus ($|r|=0.32–0.40$, $q<0.05$), and cuneus, pericalcarine cortex, and lingual gyrus ($|r|=0.38–0.47$, $q<0.05$). A significant association was also observed between variability of linear drawing velocity on the figure-of-8 and the cervical spinal cord area ($r=-0.44$, $q<0.05$).

Similarly, for each correlation observed with the 9HPT, at least one Pinching Test measure was significantly associated with the same MRI outcome, except for the cerebral white matter (Figs. 2, 3b). Some correlations, however, were observed only with the Pinching Test. This includes correlations between longer double touch asynchrony and smaller volumes of the pons ($r=-0.35$, $q<0.05$), thalamus ($r=-0.41$, $q<0.05$), hippocampus ($r=-0.45$, $q<0.05$), and interestingly with a larger volume of the anterior cingulate cortex ($r=0.36$, $q<0.05$). Additionally, longer gap duration between pinches was also associated with a smaller volume of the thalamus ($r=-0.36$, $q<0.05$), insula ($r=-0.32$, $q<0.05$), and the cuneus, pericalcarine cortex, and lingual gyrus ($r=-0.35$, $q<0.05$).

On the SBT, larger sway path correlated with a smaller volume of the paracentral lobule ($r=-0.42$, $q<0.05$; Figs. 2, 3c). In contrast, a lower total score on the Berg Balance Scale (worse ability to balance) correlated mostly with smaller volumes of deep gray matter structures ($r=0.39-0.44$ for correlations with $q<0.05$; Figs. 2, 3c).

No correlations with any of the regional MRI outcomes were found for any of the gait tests, neither for the digital measures derived from the 2MWT/UTT nor for the T25FW (Fig. 2; all $q\geq0.05$).

Next, the variance observed in the digital measures that can be explained by structural MRI outcomes was estimated using a Bayesian ridge regression model. Up to a third of the

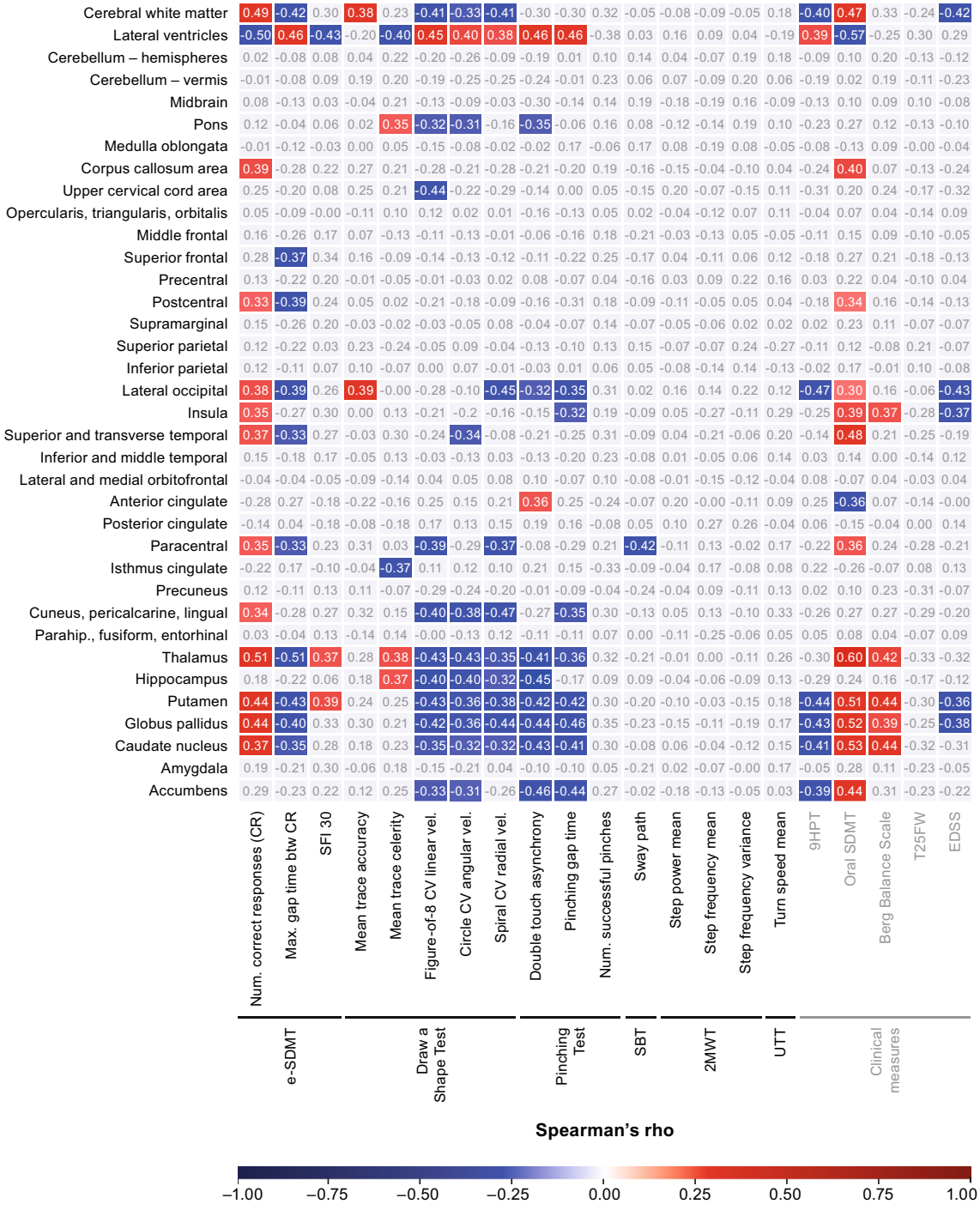

Fig. 2 Spearman's rank correlation analysis of digital measures and standard clinical measures with global and regional MRI outcomes. Statistically significant ($q < 0.05$) positive and negative correlations are highlighted in red and blue, respectively. FDR correction was applied for each digital and standard clinical measure separately to correct for multiple comparisons. Higher values equate to better performance on the oral SDMT and Berg Balance Scale, as well as for digital measures assessing number of correct responses and SFI 30 on the e-SDMT; trace accuracy and trace celerity on the Draw a Shape Test; number of pinches on the Pinching Test; mean step power and mean step frequency on the 2MWT; and mean turn speed on the UTT. In contrast, higher values equate to worse performance on the EDSS, 9HPT, and T25FW, as well as for digital measures assessing max. gap time between correct responses on the e-SDMT; CV linear, angular, and radial velocity on the Draw a Shape Test; double touch asynchrony and pinching gap time on the Pinching Test; sway path on the SBT; and step frequency variance on the 2MWT. *2MWT* Two-Minute Walk Test, *9HPT* Nine-Hole Peg Test, *btw* between, *CR* correct responses, *CV* coefficient of variation, *EDSS* Expanded Disability Status Scale, *e-SDMT* smartphone-based electronic Symbol Digit Modalities Test, *FDR* false discovery rate, *num.* number of, *parahip.* parahippocampus, *SBT* Static Balance Test, *SDMT* Symbol Digit Modalities Test, *SFI* speed fatigability index, *T25FW* Timed 25-Foot Walk, *UTT* U-Turn Test, *vel.* drawing velocity

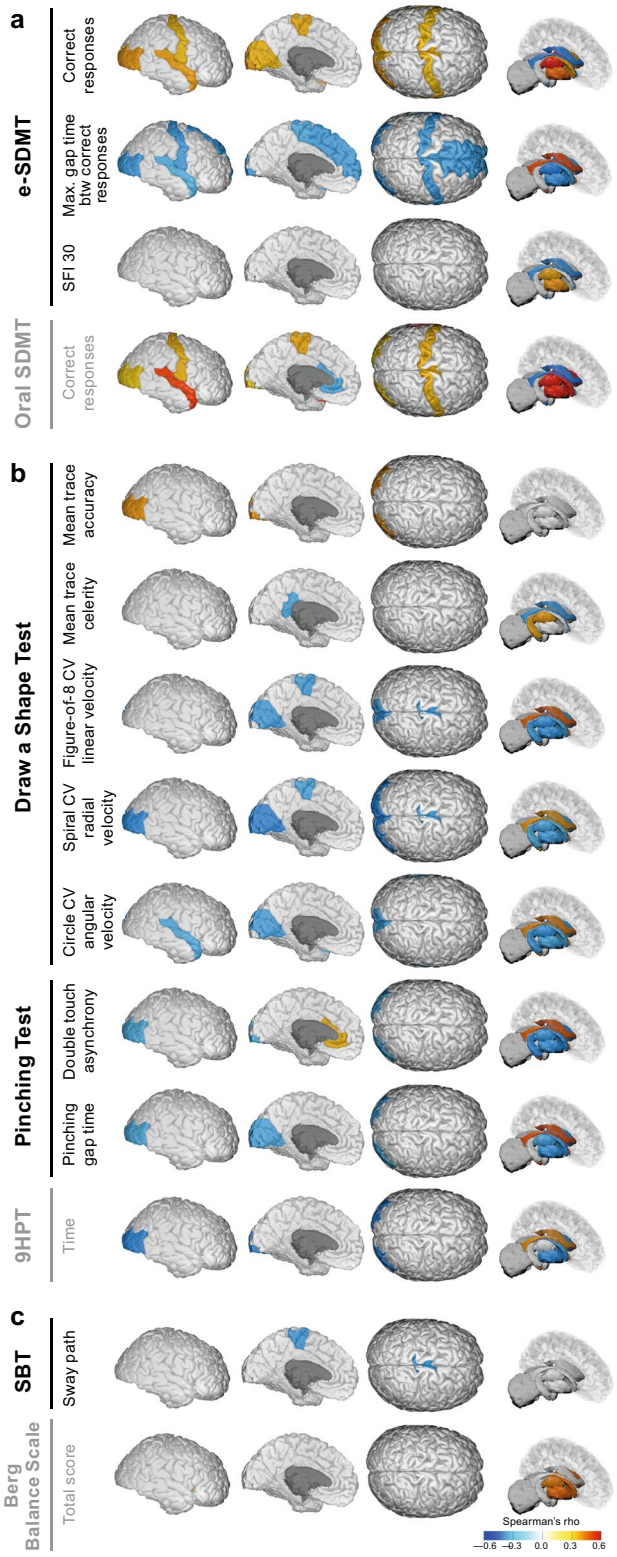

variance observed in the digital measures ($R^2 = 34\%$) could be explained when using either normalized total brain volume as individual predictor ("Whole Brain" model) or volumetric data from the 36 individual MRI regions as multiple predictors ("Parcellation" model). In the upper extremity function domain, however, comparable or higher R^2 values were obtained with the Parcellation model compared with the Whole Brain model. This suggests that multiple predictors, thus multiple brain regions, can explain as much or more of the observed variance in the digital measures (Figs. 4, SI6b). The increase in R^2 was most noticeable for mean trace celerity ($R^2 = 0.23$ vs. 0), spiral coefficient of variation (CV) linear drawing velocity ($R^2 = 0.22$ vs. 0.02), figure-of-8 CV linear drawing velocity ($R^2 = 0.19$ vs. 0.12), and double-touch asynchrony ($R^2 = 0.16$ vs. 0.06, respectively, for the Parcellation vs. Whole Brain model). This was also reflected by a less uniform distribution of the individual Bayesian ridge regression coefficients across the 36 MRI regions (Fig. SI7). By comparison, the R^2 score was more comparable across the two models for the standard clinical measure 9HPT ($R^2 = 0.28$ vs. 0.25) (Fig. 4).

Discussion

Digital measures captured by the Floodlight PoC app demonstrated robust correlations with volumetric measurements of specific brain regions. While many neural correlates were shared between clinical and digital measures, the latter showed associations with brain regions that clinical measures were unable to demonstrate. These results indicate that remotely administered digital tests may yield higher functional specificity and provide potential novel information on functional ability compared with standard clinical measures. Of note, these correlations were observed in an early, relapsing cohort of PwMS,

◀ **Fig. 3** Spearman's rank correlations adjustment for age, sex, and BMI. Statistically significant ($q < 0.05$) correlations between regional brain volume measured by MRI and measures of **a** the cognitive domain, **b** upper extremity function domain, and **c** balance domain are shown for four planes (from left to right: cortical outer, inner, top, and subcortical). FDR correction was applied for each digital and standard clinical measure separately to correct for multiple comparisons. Higher values equate to better performance for digital measures assessing number of correct responses and SFI 30 on the e-SDMT; trace accuracy and trace celerity on the Draw a Shape Test; and double touch asynchrony on the Pinching Test. In contrast, higher values equate to worse performance for digital measures assessing max. gap time between correct responses on the e-SDMT; CV linear, angular, and radial velocity on the Draw a Shape Test; pinching gap time on the Pinching Test; and sway path on the SBT. *9HPT* Nine-Hole Peg Test, *BMI* body mass index, *btw* between, *CV* coefficient of variation, *e-SDMT* smartphone-based electronic Symbol Digit Modalities Test, *FDR* false discovery rate, *SBT* Static Balance Test, *SDMT* Symbol Digit Modalities Test, *SFI* speed fatigability index

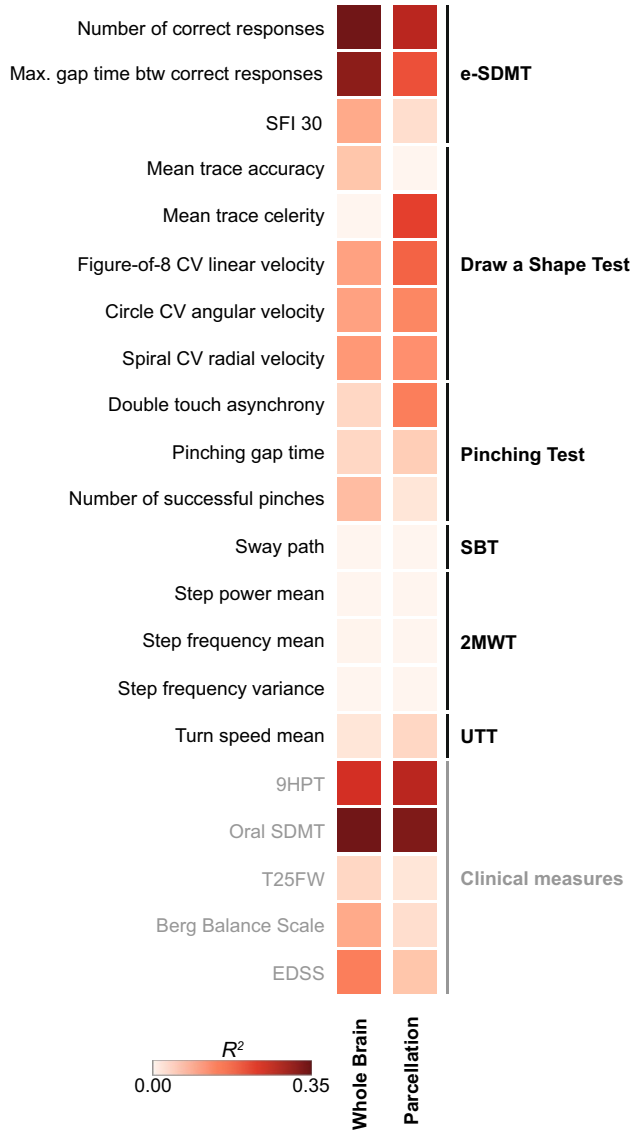

Fig. 4 Bayesian ridge regression model with leave-one-out cross validation for estimating the variance (R^2) in the digital measures and standard clinical measures that can be explained by volumetric MRI. Two models were applied. The first model ("Whole Brain") included normalized brain volume and the three demographic variables: age, sex, and body mass index (top row). The second model ("Parcellation") included all 36 regional MRI regions and the same three demographic variables (bottom row). Compared with the standard clinical measures, the digital measures tend to have a larger R^2 score in the Parcellation model vs. in the Whole Brain model, which may reflect higher functional specificity. This is particularly evident on the Draw a Shape Test (mean trace celerity and spiral CV radial velocity) and on the Pinching Test (double touch asynchrony). *2MWT* Two-Minute Walk Test, *9HPT* Nine-Hole Peg Test, *btw* between, *CV* coefficient of variation, *EDSS* Expanded Disability Status Scale, *e-SDMT* smartphone-based electronic Symbol Digit Modalities Test, *SBT* Static Balance Test, *SDMT* Symbol Digit Modalities Test, *SFI* speed fatigability index, *T25FW* Timed 25-Foot Walk, *UTT* U-Turn Test

suggesting that digital measures hold potential to capture silent pathology [31]. If confirmed in future work, this would address a key unmet need in MS disease management [32].

As expected, both the e-SDMT and oral SDMT correlated with regions implicated in cognitive decline (ventricular expansion and smaller volume of the insula and cerebral white matter), information processing speed (deep gray matter), and working memory (superior temporal gyrus) [33–39]. Correlations were also observed with the volume of the primary somatosensory cortex (postcentral gyrus) and visual processing areas (lateral occipital lobe) [34, 40]. Similarly, the Draw a Shape Test, Pinching Test, and 9HPT were associated with areas of visual processing (lateral occipital lobe, deep gray matter) and cognitive decline (ventricular expansion, cerebral white matter) [34–36]. For the SBT, postural control (sway path) correlated inversely with the paracentral lobule volume. This is consistent with findings from a functional imaging study, which suggested a role of the paracentral lobule in proprioceptive processing [41]. In contrast, the Berg Balance Scale correlated more strongly with the deep gray matter volume. The different tasks involved in the two tests, the distinctive sensorimotor aspects they capture, and the scoring—the SBT measures the total sway path (a measure of static balance), while the Berg Balance Scale provides an overall score describing both static and dynamic balance—may explain these differences. The mild level of MS-related impairment together with the ceiling effect observed on the Berg Balance Scale may have contributed to the lack of correlations with the cerebellar volume. The former may also explain the lack of correlations found for the sensor-based walking tests (UTT, 2MWT) or the T25FW [42]. With greater levels of impairment, correlations between the T25FW and thalamic volumes or upper cervical cord area could be expected [43, 44].

Several correlations were only observed for the digital measures, but not for the standard clinical measures. This was most evident in the upper extremity function domain. Temporal and spatiotemporal measures derived from the Draw a Shape Test such as the mean trace celerity and variability of drawing velocity while drawing round shapes specifically correlated with thalamic volume, which has been previously shown to be involved in information processing [45]. These measures also specifically correlated with the volume of the pons. Brainstem atrophy is reported in early stages of MS and a higher pontine lesion load has been associated with upper extremity tremor [7, 46]. In addition, the variability of linear drawing velocity on the figure-of-8 specifically correlated with the upper cervical cord area. This region has been previously linked to upper extremity dysfunction, particularly in more advanced or progressive disease where atrophy is more pronounced [44, 47]. The fact

that we observed this correlation in a mildly impaired cohort highlights the potential higher sensitivity of Floodlight PoC digital measures. Correlations specific to the digital measures were also observed with the Pinching Test. Double touch asynchrony, that corresponds to an asynchronous contact of the two fingers with the touchscreen while pinching a tomato, was associated with the volume of anterior cingulate cortex. No association was observed with the 9HPT time. This region is known to selectively modulate motor areas during visually coordinated tasks [48, 49]. This result is not surprising considering that double touch asynchrony was specifically developed to assess the ability to perform finger coordination tasks.

The notion that digital measures may offer higher functional specificity is also supported by the explained variance analysis. A low R^2 value in the Whole Brain model but a high R^2 value in the Parcellation model indicates that certain regions contribute more than other regions to the variance observed in the digital or standard clinical measures. This can be seen in the upper extremity function domain, where selected measures derived from the Draw a Shape and Pinching Tests showed a larger increase in R^2 when switching from the Whole Brain to the Parcellation model compared with the 9HPT. This suggests that these digital measures have higher functional specificity than the 9HPT. A high R^2 value in both models, on the other hand, indicates that the different MRI regions contribute equally to the observed variance. The cognitive domain with both the e-SDMT and oral SDMT is a good example of this, with both showing comparable functional specificity.

There are some limitations to this study. First, MRI data were only collected for PwMS. Consequently, we were unable to disentangle physiologic from pathologic effects. Second, the relatively short study duration of 24 weeks did not allow us to perform longitudinal analyses or assess the relationship between the digital measures and disease progression. Third, PwMS enrolled in this study mostly had mild disease with limited functional impairment, which may have weakened the correlations. Structural, or even functional, cortical reorganization, that helps to maintain functional ability in early stages of the disease despite structural damage to the brain [50–53], may have further weakened the observed correlations. Finally, spurious correlations cannot be excluded. However, the observed effects remained largely statistically significant even when applying a more conservative correction for multiple testing (FDR correction applied for all the possible combinations of the 36 anatomical regions and 21 digital/clinical measures [36 × 21 configuration]), suggesting that potential spurious correlations are negligible (Fig. SI8).

In the future, using data from larger, ongoing, and forthcoming studies (CONSONANCE, NCT03523858; Floodlight™ MS—TONiC, ISRCTN11088592), we will explore both cortical and subcortical structural networks [54, 55] and assess the relationship between longitudinal changes in digital measures and MRI outcomes to better characterize the utility of sensor-based tests as prognostic biomarkers. Such biomarkers could be used for early identification of patients with silent progression at risk of future disability accrual, and optimization of individual treatment strategies.

Conclusions

In this exploratory post-hoc analysis, digital measures obtained with the Floodlight PoC app correlated with normalized volumes of distinct anatomical regions. While many of the correlations were also observed with standard clinical measures, some were only observed with the digital measures. In addition, the explained variance analysis may suggest a higher functional specificity for digital measures, in particular in the upper extremity function domain. These results indicate that digital measures, by leveraging sensor technology, can probe multiple different neurologic domains rather than just providing an overall assessment of functional ability. Thus, digital measures have the potential to complement standard clinical measures by providing a more detailed picture of MS and a more accessible assessment of functional ability. Larger, ongoing, and forthcoming studies will need to confirm these preliminary findings.

Supplementary Information The online version contains supplementary material available at https://doi.org/10.1007/s00415-022-11494-0.

Acknowledgements We would like to thank all patients, their families, and the investigators who participated in this trial. We would like to thank the following colleagues at F. Hoffmann-La Roche Ltd for their contributions and support to the study: Jan Beckmann, Sandro Fritz, Nicholas Pierce Heinemeier, Timothy Kilchenmann, Lito Kriara, Grégoire Pointeau, Cedric Simillion, Jens Schjodt-Eriksen, Jörg Sprengel, and Mattia Zanon. Writing and editorial assistance for this manuscript was provided by Terri Desmonds, PhD, from Articulate Science, United Kingdom, and funded by F. Hoffmann-La Roche Ltd.

Author contributions Design or conceptualization of the study: CB, ML. Analysis or interpretation of the data: MG, JSG, SPH, FD, LG, LC. Drafting and revising the manuscript for intellectual content: MG, JSG, SPH, FD, LM, LG, LC, FL, CB, XM, SLH, ML.

Funding This research was funded by F. Hoffmann-La Roche Ltd, Basel, Switzerland.

Data availability For up-to-date details on Roche's Global Policy on Sharing of Clinical Study Information and how to request access to related clinical study documents, see here: https://go.roche.com/data_sharing. Request for the data underlying this publication requires a detailed, hypothesis-driven, statistical analysis plan that is collaboratively developed by the requestor and company subject matter experts. Such requests should be directed to dbm.datarequest@roche.com for consideration. Anonymized records for individual patients across more than one data source external to Roche cannot, and should not, be linked due to a potential increase in risk of patient re-identification.

Declarations

Conflicts of interest MG is a contractor for F. Hoffmann-La Roche Ltd. JSG over the past year has received grant/contract research support from the National MS Society, Biogen, and Octave Biosciences. She serves on a steering committee for a trial supported by Novartis. She has received honoraria for a non-promotional, educational activity for Sanofi Genzyme. She has received speaker fees from Alexion and BMS and served on an advisory board for Genentech. SPH is a contractor for F. Hoffmann-La Roche Ltd. FD was an employee of and is a shareholder in F. Hoffmann-La Roche Ltd; he is currently employed by Novartis Institutes for Biomedical Research. LM has nothing to disclose. LG is an employee of F. Hoffmann-La Roche Ltd. LC is an employee of and shareholder in F. Hoffmann-La Roche Ltd. FL is an employee of F. Hoffmann-La Roche Ltd. CB is a contractor for F. Hoffmann-La Roche Ltd. XM has received speaking honoraria and travel expenses for participation in scientific meetings; has been a steering committee member of clinical trials; or participated in advisory boards of clinical trials in the past years with Actelion, Alexion, Bayer, Biogen, Celgene, EMD Serono, Genzyme, Immunic, Medday, Merck, Mylan, Nervgen, Novartis, Roche, Sanofi-Genzyme, Teva, TG Therapeutics, Excemed, MSIF, and NMSS. SLH serves on the scientific advisory boards for Alector, Annexon, and Accure; is on the Board of Directors for Neurona Therapeutics; and has received travel reimbursement and writing assistance from F. Hoffmann-La Roche Ltd and Novartis for CD20-related meetings and presentations. ML is a consultant for F. Hoffmann-La Roche Ltd via Inovigate.

Ethics approval The study was registered on clinicaltrials.gov (NCT02952911). The study was conducted in full conformance with the ICH E6 guideline for Good Clinical Practice and the principles of the Declaration of Helsinki. All participants provided informed consent and ethical approval was obtained from the ethics committee of the Vall d'Hebron University Hospital, Barcelona, Spain (study number: PR(AG)300/2016) and the institutional review board of the University of California San Francisco, San Francisco, CA, USA (reference number: 175728) prior to study initiation.

Open Access This article is licensed under a Creative Commons Attribution 4.0 International License, which permits use, sharing, adaptation, distribution and reproduction in any medium or format, as long as you give appropriate credit to the original author(s) and the source, provide a link to the Creative Commons licence, and indicate if changes were made. The images or other third party material in this article are included in the article's Creative Commons licence, unless indicated otherwise in a credit line to the material. If material is not included in the article's Creative Commons licence and your intended use is not permitted by statutory regulation or exceeds the permitted use, you will need to obtain permission directly from the copyright holder. To view a copy of this licence, visit http://creativecommons.org/licenses/by/4.0/.

References

1. Reich DS, Lucchinetti CF, Calabresi PA (2018) Multiple sclerosis. N Engl J Med 378:169–180. https://doi.org/10.1056/NEJMra1401483
2. Steenwijk MD, Geurts JJ, Daams M et al (2016) Cortical atrophy patterns in multiple sclerosis are non-random and clinically relevant. Brain 139(Pt 1):115–126. https://doi.org/10.1093/brain/awv337
3. D'Ambrosio A, Pagani E, Riccitelli GC et al (2017) Cerebellar contribution to motor and cognitive performance in multiple sclerosis: an MRI sub-regional volumetric analysis. Mult Scler 23:1194–1203. https://doi.org/10.1177/1352458516674567
4. Schlaeger R, Papinutto N, Panara V et al (2014) Spinal cord gray matter atrophy correlates with multiple sclerosis disability. Ann Neurol 76:568–580. https://doi.org/10.1002/ana.24241
5. Pagani E, Rocca MA, Gallo A et al (2005) Regional brain atrophy evolves differently in patients with multiple sclerosis according to clinical phenotype. AJNR Am J Neuroradiol 26:341–346
6. Eshaghi A, Prados F, Brownlee WJ et al (2018) Deep gray matter volume loss drives disability worsening in multiple sclerosis. Ann Neurol 83:210–222. https://doi.org/10.1002/ana.25145
7. Eshaghi A, Marinescu RV, Young AL et al (2018) Progression of regional grey matter atrophy in multiple sclerosis. Brain 141:1665–1677. https://doi.org/10.1093/brain/awy088
8. Cordani C, Hidalgo de la Cruz M, Meani A et al (2020) MRI correlates of clinical disability and hand-motor performance in multiple sclerosis phenotypes. Mult Scler 27:1205–1221. https://doi.org/10.1177/1352458520958356
9. Artemiadis A, Anagnostouli M, Zalonis I et al (2018) Structural MRI correlates of cognitive function in multiple sclerosis. Mult Scler Relat Disord 21:1–8. https://doi.org/10.1016/j.msard.2018.02.003
10. Jakimovski D, Weinstock-Guttman B, Hagemeier J et al (2018) Walking disability measures in multiple sclerosis patients: correlations with MRI-derived global and microstructural damage. J Neurol Sci 393:128–134. https://doi.org/10.1016/j.jns.2018.08.020
11. Mistri D, Cacciaguerra L, Storelli L et al (2022) The association between cognition and motor performance is beyond structural damage in relapsing-remitting multiple sclerosis. J Neurol 269:4213–4221. https://doi.org/10.1007/s00415-022-11044-8
12. Sormani MP, De Stefano N, Giovannoni G et al (2019) Learning ability correlates with brain atrophy and disability progression in RRMS. J Neurol Neurosurg Psychiatry 90:38–43. https://doi.org/10.1136/jnnp-2018-319129
13. Montalban X, Graves J, Midaglia L et al (2022) A smartphone sensor-based digital outcome assessment of multiple sclerosis. Mult Scler 28:654–664. https://doi.org/10.1177/13524585211028561
14. Midaglia L, Mulero P, Montalban X et al (2019) Adherence and satisfaction of smartphone- and smartwatch-based remote active testing and passive monitoring in people with multiple sclerosis: nonrandomized interventional feasibility study. J Med Internet Res 21:e14863. https://doi.org/10.2196/14863
15. Polman CH, Reingold SC, Banwell B et al (2011) Diagnostic criteria for multiple sclerosis: 2010 revisions to the McDonald criteria. Ann Neurol 69:292–302. https://doi.org/10.1002/ana.22366
16. Kurtzke JF (1983) Rating neurologic impairment in multiple sclerosis: an Expanded Disability Status Scale (EDSS). Neurology 33:1444–1452. https://doi.org/10.1212/wnl.33.11.1444
17. Jain S, Sima DM, Ribbens A et al (2015) Automatic segmentation and volumetry of multiple sclerosis brain lesions from MR images. Neuroimage Clin 8:367–375. https://doi.org/10.1016/j.nicl.2015.05.003
18. Rakić M, Vercruyssen S, Van Eyndhoven S et al (2021) icobrain ms 5.1: combining unsupervised and supervised approaches for improving the detection of multiple sclerosis lesions. Neuroimage Clin 31:102707. https://doi.org/10.1016/j.nicl.2021.102707
19. Sastre-Garriga J, Pareto D, Battaglini M et al (2020) MAGNIMS consensus recommendations on the use of brain and spinal cord atrophy measures in clinical practice. Nat Rev Neurol 16:171–182. https://doi.org/10.1038/s41582-020-0314-x
20. U.S. Food and Drug Administration (2019) Substantial equivalence determination: icobrain. Regulation Number: 21 CFR 892.2050. https://www.accessdata.fda.gov/cdrh_docs/pdf19/K192130.pdf. Accessed 13 Oct 2022

21. Struyfs H, Sima DM, Wittens M et al (2020) Automated MRI volumetry as a diagnostic tool for Alzheimer's disease: validation of icobrain dm. Neuroimage Clin 26:102243. https://doi.org/10.1016/j.nicl.2020.102243
22. Steenwijk MD, Amiri H, Schoonheim MM et al (2017) Agreement of MSmetrix with established methods for measuring cross-sectional and longitudinal brain atrophy. Neuroimage Clin 15:843–853. https://doi.org/10.1016/j.nicl.2017.06.034
23. Liu Y, Lukas C, Steenwijk M et al (2016) Multicenter validation of mean upper cervical cord area measurements from head 3D T1-weighted MR imaging in patients with multiple sclerosis. AJNR Am J Neuroradiol 37:749–754. https://doi.org/10.3174/ajnr.A4635
24. Liu Z, Yaldizli Ö, Pardini M et al (2015) Cervical cord area measurement using volumetric brain magnetic resonance imaging in multiple sclerosis. Mult Scler Relat Disord 4:52–57. https://doi.org/10.1016/j.msard.2014.11.004
25. Van Hecke W, Billiet T, Pedrosa de Barros N et al (2019) Evaluation of spinal cord atrophy in different MS subtypes using icospine. In: Poster presented at: 37th Congress of the European Committee for Treatment and Research in Multiple Sclerosis; September 11–13; Stockholm, Sweden
26. Pedrosa de Barros N, Billiet T, Denissen S et al (2020) Assessing cervical spinal cord atrophy in T1-weighted brain scans using icobrain. In: Poster presented at: American Society of Neuroimaging 43rd Annual Meeting; March 5–7; Atlanta, GA, USA
27. De Leener B, Lévy S, Dupont SM et al (2017) SCT: Spinal Cord Toolbox, an open-source software for processing spinal cord MRI data. Neuroimage Clin 145:24–43. https://doi.org/10.1016/j.neuroimage.2016.10.009
28. Huber PJ (1981) Robust statistics. Wiley, New York
29. Benjamini Y, Hochberg Y (1995) Controlling the false discovery rate: a practical and powerful approach to multiple testing. J R Statist Soc B 57:289–300. https://doi.org/10.1111/j.2517-6161.1995.tb02031.x
30. MacKay DJC (1992) Bayesian interpolation. Neural Comput 4:415–447. https://doi.org/10.1162/neco.1992.4.3.415
31. University of California San Francisco MS-EPIC Team, Cree BA, Hollenbach JA et al (2019) Silent progression in disease activity-free relapsing multiple sclerosis. Ann Neurol 85:653–666. https://doi.org/10.1002/ana.25463
32. Members of the MS in the 21st Century Steering Group, Rieckmann P, Centonze D et al (2018) Unmet needs, burden of treatment, and patient engagement in multiple sclerosis: a combined perspective from the MS in the 21st Century Steering Group. Mult Scler Relat Disord 19:153–160. https://doi.org/10.1016/j.msard.2017.11.013
33. Achiron A, Chapman J, Tal S, Bercovich E, Gil H (2013) Superior temporal gyrus thickness correlates with cognitive performance in multiple sclerosis. Brain Struct Funct 218:943–950. https://doi.org/10.1007/s00429-012-0440-3
34. Bisecco A, Stamenova S, Caiazzo G et al (2018) Attention and processing speed performance in multiple sclerosis is mostly related to thalamic volume. Brain Imaging Behav 12:20–28. https://doi.org/10.1007/s11682-016-9667-6
35. Carmichael OT, Kuller LH, Lopez OL et al (2007) Cerebral ventricular changes associated with transitions between normal cognitive function, mild cognitive impairment, and dementia. Alzheimer Dis Assoc Disord 21:14–24. https://doi.org/10.1097/WAD.0b013e318032d2b1
36. Engl C, Tiemann L, Grahl S et al (2020) Cognitive impairment in early MS: contribution of white matter lesions, deep grey matter atrophy, and cortical atrophy. J Neurol 267:2307–2318. https://doi.org/10.1007/s00415-020-09841-0
37. Matías-Guiu JA, Cortés-Martínez A, Montero P et al (2018) Identification of cortical and subcortical correlates of cognitive performance in multiple sclerosis using voxel-based morphometry. Front Neurol 9:920. https://doi.org/10.3389/fneur.2018.00920
38. Zhang X, Zhang F, Huang D et al (2016) Contribution of gray and white matter abnormalities to cognitive impairment in multiple sclerosis. Int J Mol Sci 18:46. https://doi.org/10.3390/ijms18010046
39. Batista S, Zivadinov R, Hoogs M et al (2012) Basal ganglia, thalamus and neocortical atrophy predicting slowed cognitive processing in multiple sclerosis. J Neurol 259:139–146. https://doi.org/10.1007/s00415-011-6147-1
40. Riccitelli GC, Pagani E, Rodegher M et al (2019) Imaging patterns of gray and white matter abnormalities associated with PASAT and SDMT performance in relapsing-remitting multiple sclerosis. Mult Scler 25:204–216. https://doi.org/10.1177/1352458517743091
41. Goossens N, Janssens L, Caeyenberghs K, Albouy G, Brumagne S (2019) Differences in brain processing of proprioception related to postural control in patients with recurrent non-specific low back pain and healthy controls. Neuroimage Clin 23:101881. https://doi.org/10.1016/j.nicl.2019.101881
42. Maghzi AH, Revirajan N, Julian LJ et al (2014) Magnetic resonance imaging correlates of clinical outcomes in early multiple sclerosis. Mult Scler Relat Disord 3:720–727. https://doi.org/10.1016/j.msard.2014.07.003
43. Bergsland N, Benedict RHB, Dwyer MG et al (2021) Thalamic nuclei volumes and their relationships to neuroperformance in multiple sclerosis: a cross-sectional structural MRI study. J Magn Reson Imaging 53:731–739. https://doi.org/10.1002/jmri.27389
44. Daams M, Weiler F, Steenwijk MD et al (2014) Mean upper cervical cord area (MUCCA) measurement in long-standing multiple sclerosis: relation to brain findings and clinical disability. Mult Scler 20:1860–1865. https://doi.org/10.1177/1352458514533399
45. Merchant H, Harrington DL, Meck WH (2013) Neural basis of the perception and estimation of time. Annu Rev Neurosci 36:313–336. https://doi.org/10.1146/annurev-neuro-062012-170349
46. Feys P, Maes F, Nuttin B et al (2005) Relationship between multiple sclerosis intention tremor severity and lesion load in the brainstem. NeuroReport 16:1379–1382. https://doi.org/10.1097/01.wnr.0000176521.26971.58
47. Rocca MA, Horsfield MA, Sala S et al (2011) A multicenter assessment of cervical cord atrophy among MS clinical phenotypes. Neurology 76:2096–2102. https://doi.org/10.1212/WNL.0b013e31821f46b8
48. Asemi A, Ramaseshan K, Burgess A, Diwadkar VA, Bressler SL (2015) Dorsal anterior cingulate cortex modulates supplementary motor area in coordinated unimanual motor behavior. Front Hum Neurosci 9:309. https://doi.org/10.3389/fnhum.2015.00309
49. Paus T, Petrides M, Evans AC, Meyer E (1993) Role of the human anterior cingulate cortex in the control of oculomotor, manual, and speech responses: a positron emission tomography study. J Neurophysiol 70:453–469. https://doi.org/10.1152/jn.1993.70.2.453
50. Pantano P, Mainero C, Caramia F (2006) Functional brain reorganization in multiple sclerosis: evidence from fMRI studies. J Neuroimaging 16:104–114. https://doi.org/10.1111/j.1552-6569.2006.00029.x
51. Rocca MA, Falini A, Colombo B, Scotti G, Comi G, Filippi M (2002) Adaptive functional changes in the cerebral cortex of patients with nondisabling multiple sclerosis correlate with the extent of brain structural damage. Ann Neurol 51:330–339. https://doi.org/10.1002/ana.10120
52. Fleischer V, Gröger A, Koirala N et al (2017) Increased structural white and grey matter network connectivity compensates for functional decline in early multiple sclerosis. Mult Scler 23:432–441. https://doi.org/10.1177/1352458516651503
53. Llufriu S, Martinez-Heras E, Solana E et al (2017) Structural networks involved in attention and executive functions in multiple

sclerosis. Neuroimage Clin 13:288–296. https://doi.org/10.1016/j.nicl.2016.11.026

54. Colato E, Stutters J, Tur C et al (2021) Predicting disability progression and cognitive worsening in multiple sclerosis using patterns of grey matter volumes. J Neurol Neurosurg Psychiatry 92:995–1006. https://doi.org/10.1136/jnnp-2020-325610

55. Pagani E, Rocca MA, De Meo E et al (2020) Structural connectivity in multiple sclerosis and modeling of disconnection. Mult Scler 26:220–232. https://doi.org/10.1177/1352458518820759